Supporting Information

Stabilized Lamellar Liquid Crystalline Phase with Aggregation-Induced Emission Features Based on Pyrrolopyrrole Derivatives

Shuangxiong Dai,[a] Zhengxu Cai,[a] Zhe Peng,[a] Zhi Wang,[a] Bin Tong,[a]* Jianbing Shi,[a] Shenglong Gan,[b] Qiming He,[c] Wei Chen [b,c] and Yuping Dong [a]*

[a.] Beijing Key Laboratory of Construction Tailorable Advanced Functional Materials and Green Applications, School of Material Science & Engineering, Beijing Institute of Technology, 5 South Zhongguancun Street, Beijing, 100081, China

[b.] Materials Science Division, Argonne National Laboratory, 9700 Cass Avenue, Lemont, Illinois 60439, United States

[c.] Institute for Molecular Engineering, The University of Chicago, 5640 South Ellis Avenue, Chicago, Illinois 60637, United States

* To whom correspondence should be addressed: Phone: +86-10-6891-7390
E-mail: tongbin@bit.edu.cn, chdongyp@bit.edu.cn

Contents

S1. Synthesis and characterization of TPPP derivatives

The nine TPPP derivatives were synthesized by using the known methods.[1-2] The concrete steps are listed as follows: In a 100 mL round-bottom flask equipped with a reflux condenser and magnetic stir bar, aniline derivative (0.023 mol), benzaldehyde (2.4 g, 0.023 mol) and TsOH (0.40 g 0.0023 mol) were dissolved with 50 mL glacial acetic acid. The mixture was stirred at 90°C for 30 min. After that time, butane-2,3-dione (0.97 g, 0.0113 mol) was slowly added. Then the reaction mixture was stirred at 90°C for extra 3 h. The faint yellow precipitate of the obtained TPPP derivatives was collected by filtration. Further purification was occurred by recrystallization from $CHCl_3$ and drying in a vacuum oven to yield a yellowish powder. (Approximate yield: 11-14%)

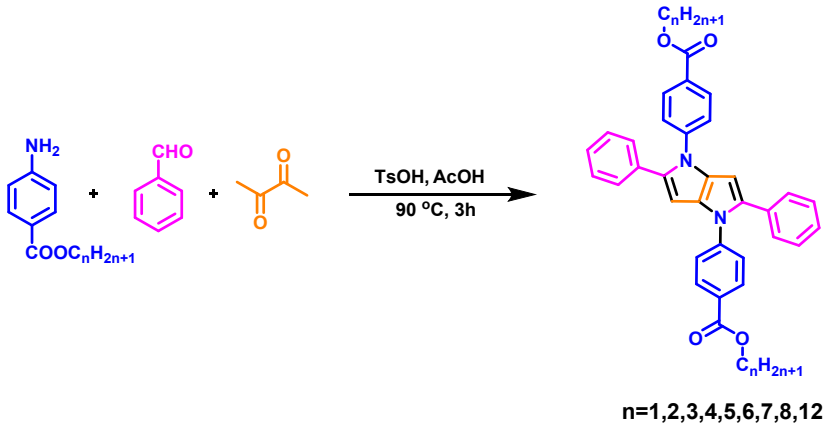

Scheme S1. The synthetic routes of the nine TPPP derivatives.

TPPP-C1: (2,5-Diphenyl-1,4-bis(4-methylbenzoat)-1,4-dihydropyrrolo[3,2-b]-pyrrole). PE/EA (2:1), yellowish powder, yield: 13%. ^{1}H NMR (400 MHz, $CDCl_3$), δ: 8.03 (d, J = 8.0 Hz, 4H), 7.32 (d, J = 8.0 Hz, 4H), 7.23 (m, 10H), 6.48 (s, 2H), 3.92 (s, 6H). ^{13}C NMR (100 MHz, $CDCl_3$), δ: (ppm): 166.56, 143.80, 136.07, 133.18, 131.28, 130.70, 128.44, 128.34, 127.03, 126.77, 124.42, 96.47, 52.20. MALDI-MS (m/z): calcd. for $C_{34}H_{26}N_2O_4$: 526.19. Found: 526.20 (M^+).

TPPP-C2: (2,5-Diphenyl-1,4-bis(4-ethylbenzoat)-1,4-dihydropyrrolo[3,2-b]-pyrrole). PE/EA (2:1), yellowish powder, yield: 14%. ^{1}H NMR (400 MHz, $CDCl_3$), δ: 8.04 (d, J = 8.0 Hz, 4H), 7.33 (d, J = 8.0 Hz, 4H), 7.24 (m, 10H), 6.47 (s, 2H), 4.38 (q, J = 8.0 Hz, 4H), 1.39 (t, J = 4.0 Hz, 6H). ^{13}C NMR (100 MHz, $CDCl_3$), δ: (ppm): 166.09, 143.72, 136.06, 133.20, 131.29, 130.65, 128.43, 128.33, 127.39, 126.74, 124.39, 96.41, 61.05, 14.36. MALDI-MS (m/z): calcd. for $C_{36}H_{30}N_2O_4$: 554.22. Found: 554.67 (M^+).

TPPP-C3: (2,5-Diphenyl-1,4-bis(4-propylbenzoat)-1,4-dihydropyrrolo[3,2-b]-pyrrole). PE/EA (3:1), yellowish powder, yield: 14%. ^{1}H NMR (400 MHz, $CDCl_3$), δ: 8.04 (d, J = 8.0 Hz, 4H), 7.32 (d, J = 8.0 Hz, 4H), 7.24 ((m, 10H), 6.47 (s, 2H), 4.28 (t, J = 8.0 Hz, 4H), 1.80 (m, 4H), 1.03 (t, J = 4.0 Hz, 6H). ^{13}C NMR (100 MHz, $CDCl_3$), δ: (ppm): 166.15, 143.72, 136.06, 133.20, 131.30, 130.66, 128.43, 128.33, 127.41, 126.74, 124.40, 96.43, 66.65, 22.15, 10.55. MALDI-MS (m/z): calcd. for $C_{38}H_{34}N_2O_4$: 582.25. Found: 582.10 (M^+).

TPPP-C4: (2,5-Diphenyl-1,4-bis(4-butylbenzoat)-1,4-dihydropyrrolo[3,2-b]-pyrrole). PE/EA (5:1), yellowish powder, yield: 13%. ^{1}H NMR (400 MHz, $CDCl_3$), δ: 8.04 (d, J = 8.0 Hz, 4H), 7.33 (d, J = 8.0 Hz, 4H), 7.23 (m, 10H), 6.47 (s, 2H), 4.33 (t, J = 4.0 Hz, 4H), 1.75 (m, 4H), 1.48 (m, 4H), 0.99 (t, J = 4.0 Hz, 6H). ^{13}C NMR (100 MHz, $CDCl_3$), δ: (ppm): 166.16, 143.72, 136.06, 133.20, 131.30, 130.65, 128.44, 128.33, 127.41, 126.74, 124.39, 96.43, 64.94, 30.82, 19.30, 13.78. MALDI-MS (m/z): calcd. for $C_{40}H_{38}N_2O_4$: 610.28. Found: 610.81 (M^+).

TPPP-C5: (2,5-Diphenyl-1,4-bis(4-amylbenzoat)-1,4-dihydropyrrolo[3,2-b]-pyrrole). PE/EA (6:1), yellowish powder, yield: 12%. ^{1}H NMR (400 MHz, $CDCl_3$), δ: 8.03 (d, J = 8.0 Hz, 4H), 7.28 (d, J = 8.0 Hz, 4H), 7.23 (m, 10H), 6.47 (s, 2H), 4.31 (t, J = 8.0 Hz, 4H), 1.77 (m, 4H), 1.41 (m, 8H), 0.94 (t, J = 8.0 Hz, 6H). ^{13}C NMR (100 MHz, $CDCl_3$), δ: (ppm): 166.15, 143.72, 136.06, 133.21, 131.31, 130.66, 128.44, 128.34, 127.43, 126.74, 124.40, 96.44, 65.25, 28.48, 28.23, 22.39, 14.00. MALDI-MS (m/z): calcd. for $C_{42}H_{42}N_2O_4$: 638.31. Found: 638.31 (M^+).

TPPP-C6: (2,5-Diphenyl-1,4-bis(4-hexylbenzoat)-1,4-dihydropyrrolo[3,2-b]-pyrrole). PE/EA (6:1), yellowish powder, yield: 11%. ^{1}H NMR (400 MHz, $CDCl_3$), δ: 8.03 (d, J = 8.0 Hz, 4H), 7.32 (d, J = 8.0 Hz, 4H), 7.24 (m, 10H), 6.47 (s, 2H), 4.31 (t, J = 8.0 Hz, 4H), 1.76 (m, 4H), 1.45 (m, 4H), 1.34 (m, 8H), 0.91 (t, J = 4.0 Hz, 6H). ^{13}C NMR (100 MHz, $CDCl_3$), δ: (ppm): 166.17, 143.70, 136.05, 133.20, 131.29, 130.66, 128.44, 128.33, 127.41, 126.74, 124.39, 96.44, 65.27, 31.50, 28.73, 25.76, 22.58, 14.05. MALDI-MS (m/z): calcd. for $C_{44}H_{46}N_2O_4$: 666.35. Found: 666.09 (M^+).

TPPP-C7: (2,5-Diphenyl-1,4-bis(4-heptylbenzoat)-1,4-dihydropyrrolo[3,2-b]-pyrrole). PE/EA (8:1), yellowish powder, yield: 11%. ^{1}H NMR (400 MHz, $CDCl_3$), δ: 8.03 (d, J = 8.0 Hz, 4H), 7.33 (d, J = 8.0 Hz, 4H), 7.23 (m, 10H), 6.48 (s, 2H), 4.31 (t, J = 8.0 Hz, 4H), 1.77 (t, J = 8.0 Hz, 4H), 1.35 (m, 16H), 0.90 (t, J = 8.0 Hz, 6H). ^{13}C NMR (100 MHz, $CDCl_3$), δ: (ppm): 166.17, 143.70, 136.05, 133.20, 131.29, 130.66, 128.44, 128.33, 127.41, 126.74, 124.39, 96.44, 65.28, 31.76, 29.00, 28.78, 26.06, 22.63, 14.10. MALDI-MS (m/z): calcd. for $C_{46}H_{50}N_2O_4$: 694.38. Found: 694.92 (M^+).

TPPP-C8: (2,5-Diphenyl-1,4-bis(4-octylbenzoat)-1,4-dihydropyrrolo[3,2-b]-pyrrole). PE/EA (8:1), yellowish powder, yield: 12%. ^{1}H NMR (400 MHz, $CDCl_3$), δ: 8.03 (d, J = 8.0 Hz, 4H), 7.32 (d, J = 8.0 Hz, 4H), 7.24 (m, 10H), 6.47 (s, 2H), 4.31 (t, J = 8.0 Hz, 4H), 1.76 (m, 4H), 1.44 (t, J = 8.0 Hz, 4H), 1.31 (m, 16H), 0.88 (t, J = 4.0 Hz, 6H). ^{13}C NMR (100 MHz, $CDCl_3$), δ: (ppm): 166.16, 143.70, 136.05, 133.20, 131.29, 130.66, 128.44, 128.33, 127.41, 126.74, 124.39, 96.43, 65.28, 31.82, 29.28, 29.22, 28.77, 26.08, 22.67, 14.12. MALDI-MS (m/z): calcd. for $C_{48}H_{54}N_2O_4$: 722.41. Found: 722.92 (M^+).

TPPP-C12: (2,5-Diphenyl-1,4-bis(4-dodecylbenzoat)-1,4-dihydropyrrolo[3,2-b]-pyrrole). PE/EA (10:1), yellowish powder, yield: 12%. ^{1}H NMR (400 MHz, $CDCl_3$), δ: 8.03 (d, J = 8.0 Hz, 4H), 7.32 (d, J = 8.0 Hz, 4H), 7.24 (m, 10H), 6.47 (s, 2H), 4.31 (t, J = 8.0 Hz, 4H), 1.76 (m, 4H), 1.43 (m, 4H), 1.36 (m, 32H), 0.88 (t, J = 4.0 Hz, 6H). ^{13}C NMR (100 MHz, $CDCl_3$), δ: (ppm):166.16, 143.70, 136.05, 133.20, 131.29, 130.66, 128.44, 128.33, 127.41, 126.74, 124.39, 96.43, 65.28, 31.93, 29.67, 29.62, 29.56, 29.37, 29.33, 28.77, 26.08, 22.71, 14.14. MALDI-MS (m/z): calcd. for $C_{56}H_{70}N_2O_4$: 834.53. Found: 834.42 (M^+).

S2. Absorption and emission spectra of the TPPP derivatives in solid states

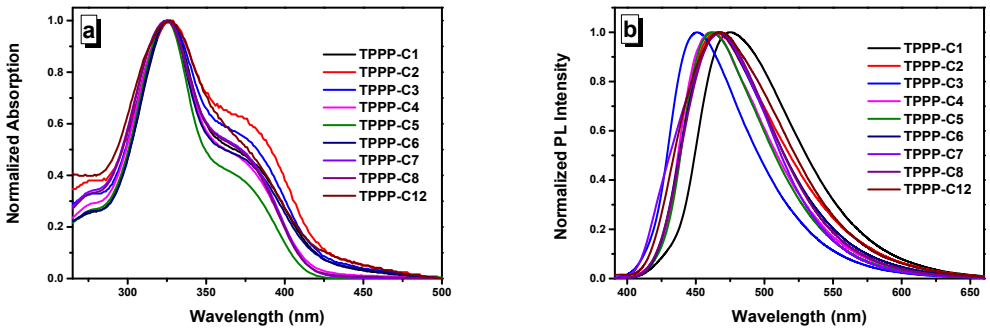

Fig. S1 (a) Normalized UV-vis absorption spectra of the TPPP derivatives in solid states; **(b)** Normalized fluorescence spectra of the TPPP derivatives in solid states.

S3. Absorption spectra of the TPPP derivatives in THF/water mixtures

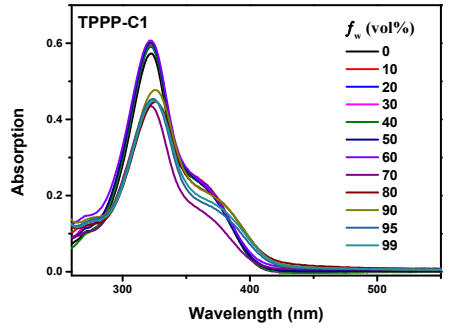

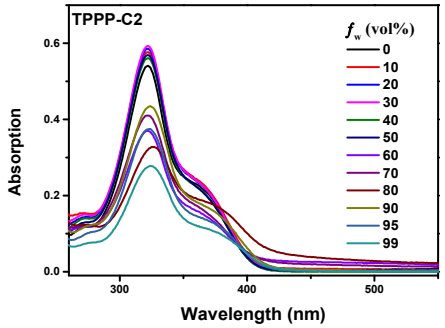

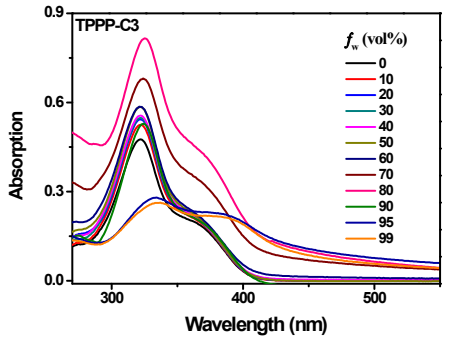

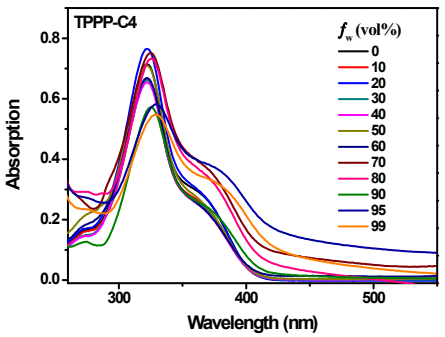

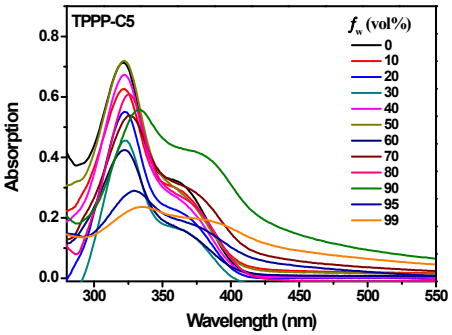

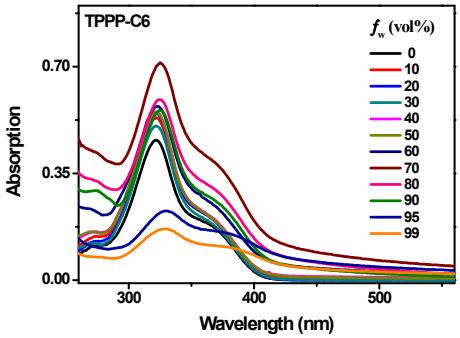

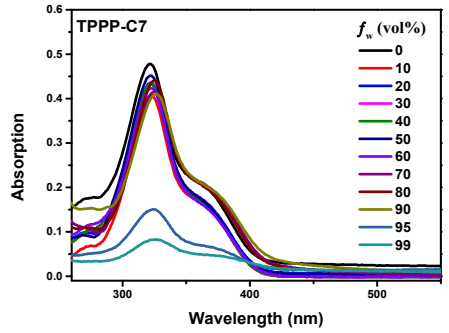

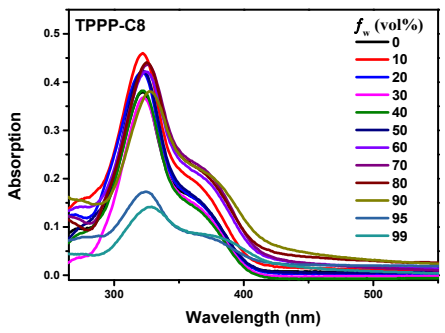

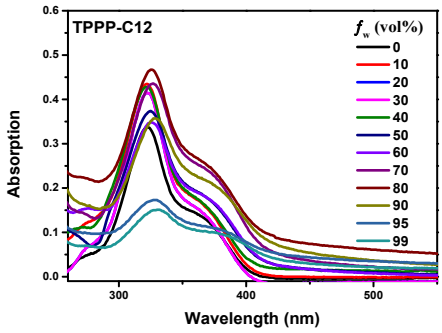

Fig. S2. UV-vis absorption spectra of the nine TPPP derivatives in THF/water mixtures with different water fractions (f_w). Concentration: 1×10^{-5} M.

S4. Emission spectra of the TPPP derivatives in THF/water mixtures

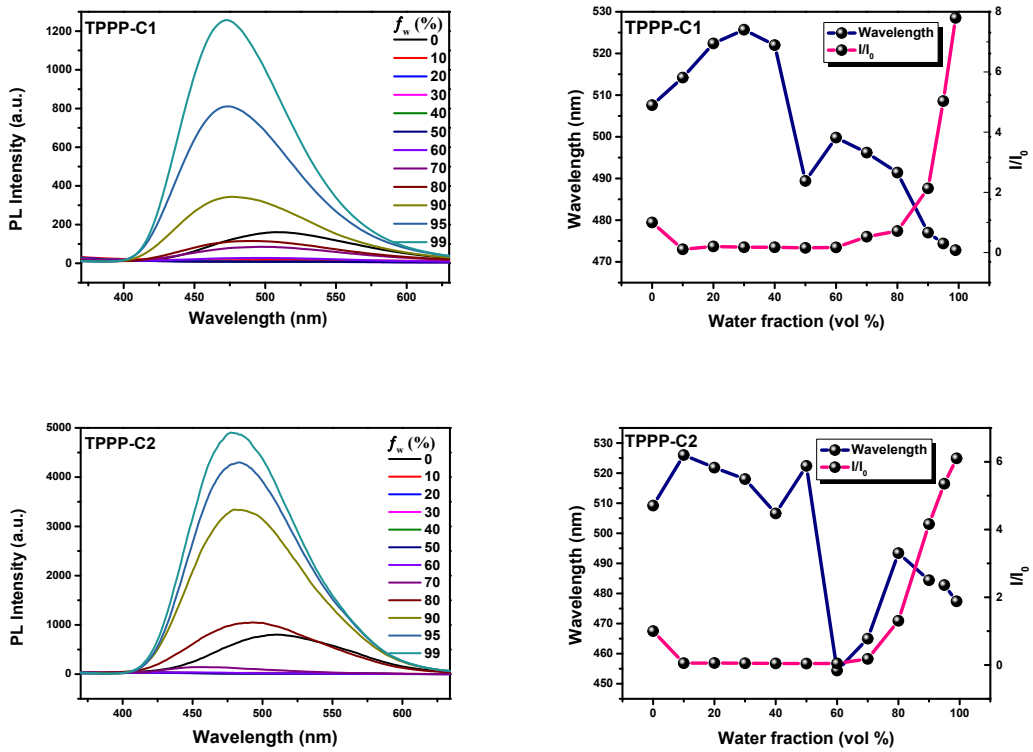

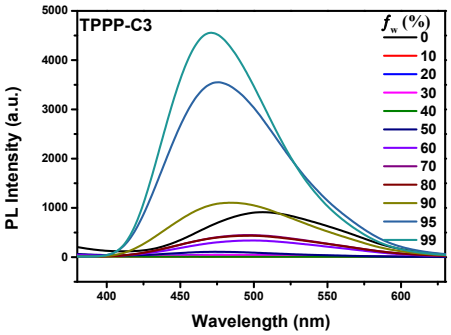
TPPP-C3
f_w (%)
0
10
20
30
40
50
60
70
80
90
95
99
PL Intensity (a.u.)
Wavelength (nm)

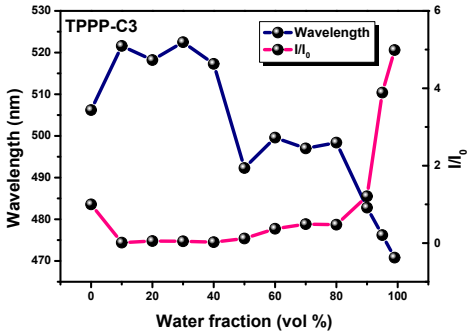
TPPP-C3
Wavelength
I/I0
Wavelength (nm)
I/I0
Water fraction (vol %)

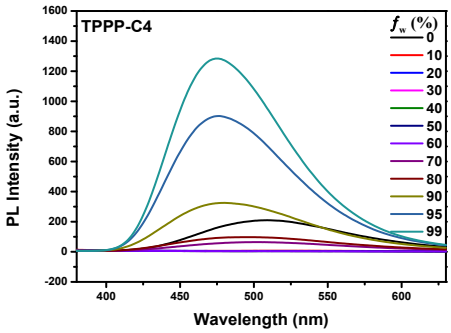
TPPP-C4
f_w (%)
0
10
20
30
40
50
60
70
80
90
95
99
PL Intensity (a.u.)
Wavelength (nm)

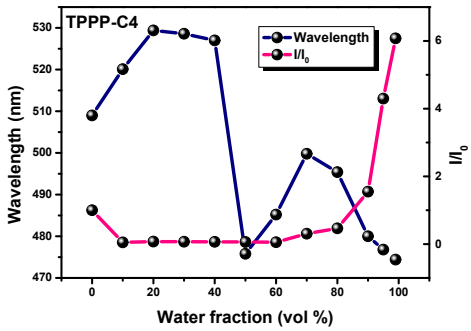
TPPP-C4
Wavelength
I/I0
Wavelength (nm)
I/I0
Water fraction (vol %)

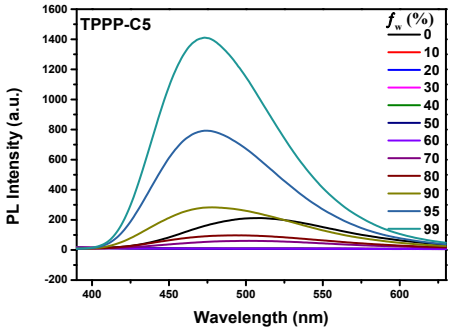
TPPP-C5
f_w (%)
0
10
20
30
40
50
60
70
80
90
95
99
PL Intensity (a.u.)
Wavelength (nm)

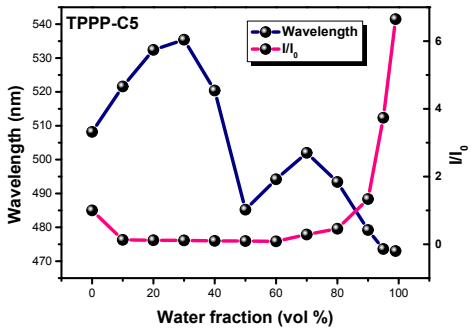
TPPP-C5
Wavelength
I/I0
Wavelength (nm)
I/I0
Water fraction (vol %)

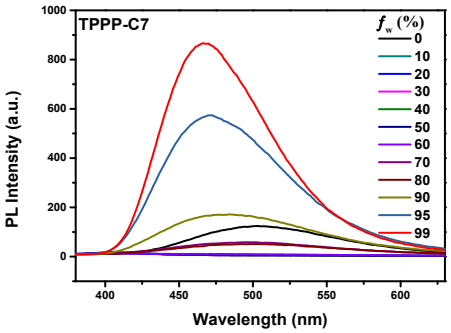
TPPP-C7
f_w (%)
0
10
20
30
40
50
60
70
80
90
95
99
PL Intensity (a.u.)
Wavelength (nm)

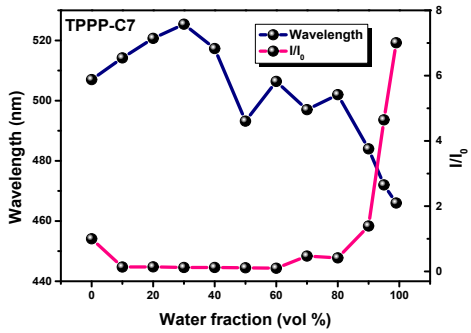
TPPP-C7
Wavelength
I/I0
Wavelength (nm)
I/I0
Water fraction (vol %)

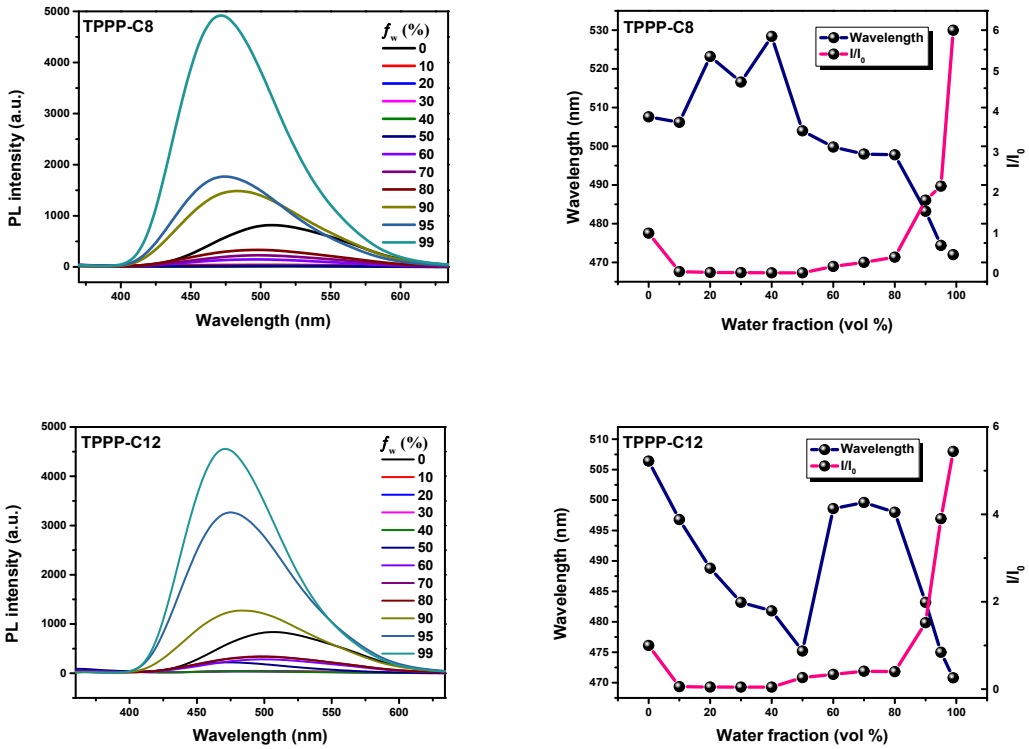

Fig. S3. Fluorescence spectra of the TPPP derivatives in THF/water mixtures with different water fractions (left); Plot of wavelength and the ratio of maximum fluorescence intensity of the TPPP derivatives vs. water fraction (right). I_0 = emission intensity in pure THF solution. Excitation wavelength: 322 nm, concentration: 1×10^{-5} M.

S5. Time-resolved PL decays spectra of the TPPP derivatives

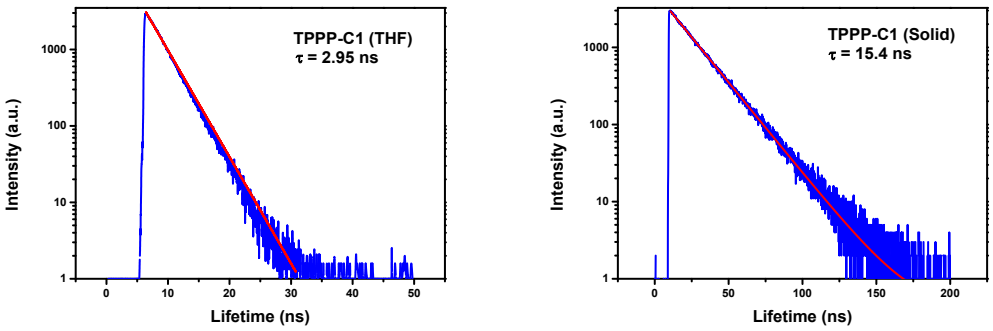

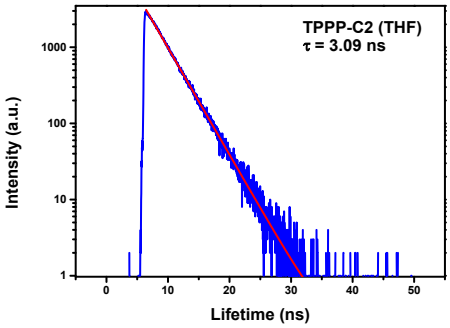
TPPP-C2 (THF)
τ = 3.09 ns
Intensity (a.u.)
Lifetime (ns)

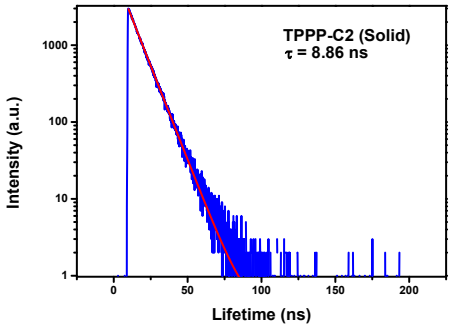
TPPP-C2 (Solid)
τ = 8.86 ns
Intensity (a.u.)
Lifetime (ns)

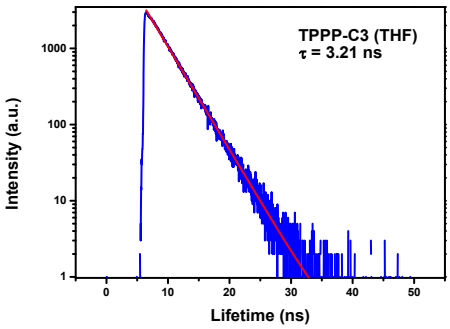
TPPP-C3 (THF)
τ = 3.21 ns
Intensity (a.u.)
Lifetime (ns)

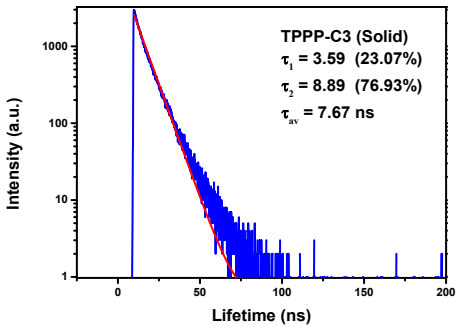
TPPP-C3 (Solid)
τ1 = 3.59 (23.07%)
τ2 = 8.89 (76.93%)
τav = 7.67 ns
Intensity (a.u.)
Lifetime (ns)

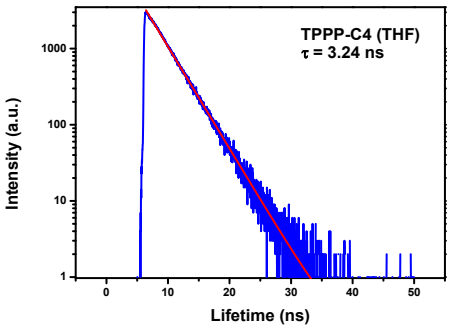
TPPP-C4 (THF)
τ = 3.24 ns
Intensity (a.u.)
Lifetime (ns)

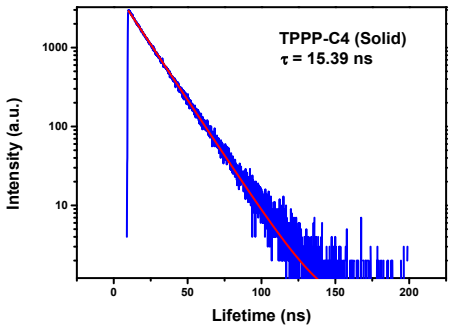
TPPP-C4 (Solid)
τ = 15.39 ns
Intensity (a.u.)
Lifetime (ns)

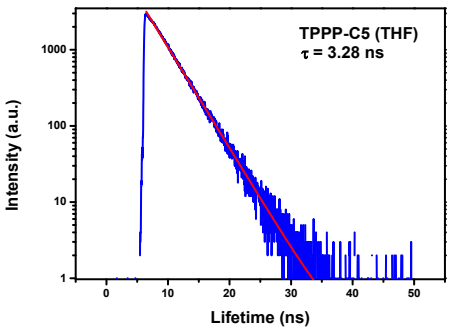
TPPP-C5 (THF)
τ = 3.28 ns
Intensity (a.u.)
Lifetime (ns)

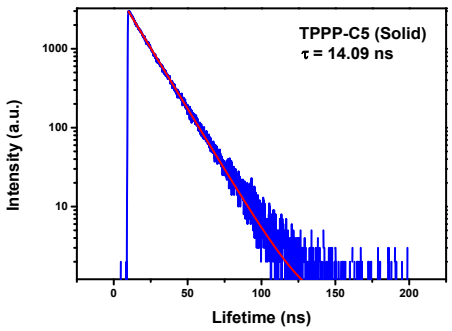
TPPP-C5 (Solid)
τ = 14.09 ns
Intensity (a.u.)
Lifetime (ns)

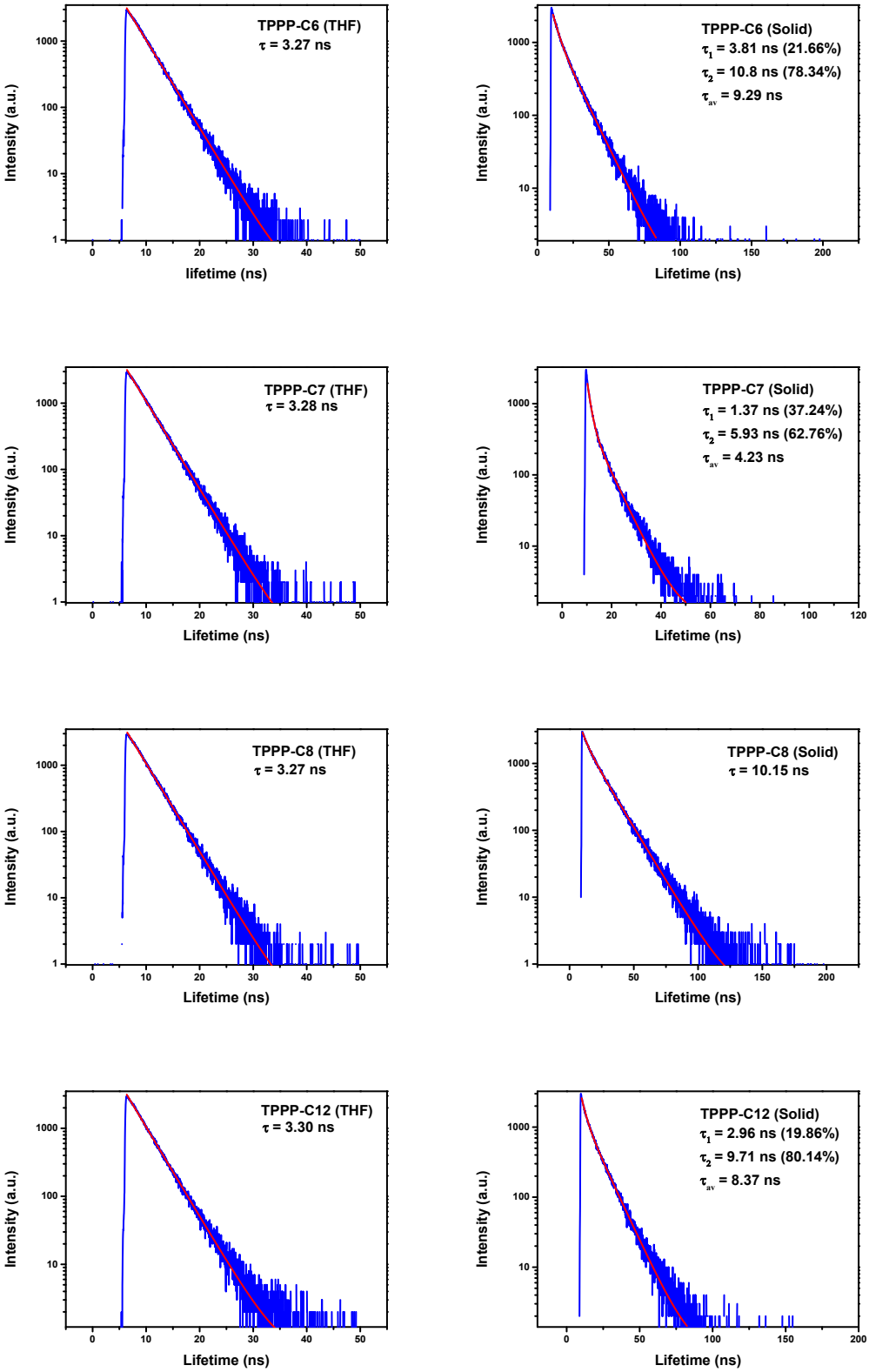

Fig. S4. Time-resolved PL decays spectra of the nine TPPP derivatives measured in THF solution (1×10^{-5} M) and solid states. All profiles were taken at room temperature.

S6. TGA test of the TPPP derivatives

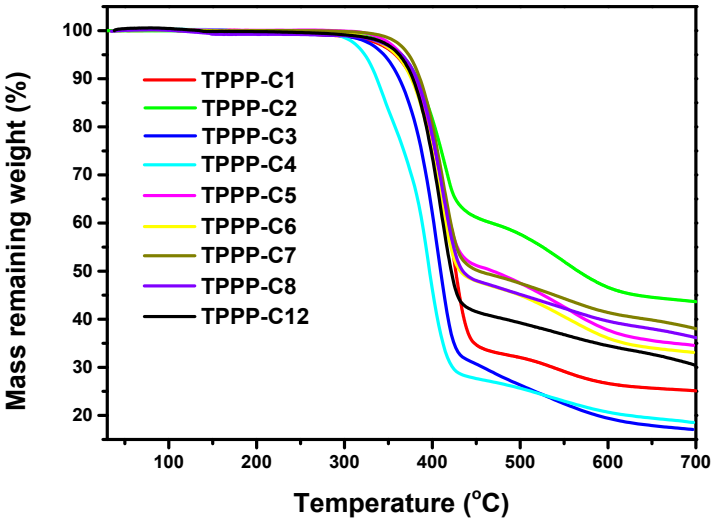

Fig. S5. TGA thermograms of the TPPP derivatives measured under nitrogen at a heating rate of 10°C/min.

S7. XRD patterns of TPPP-C6 and TPPP-C12 in the crystalline phase

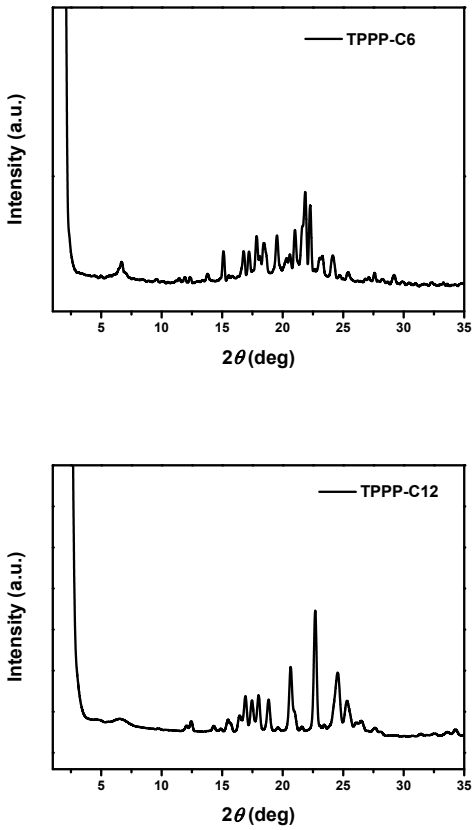

Fig. S6. XRD patterns of **TPPP-C6** and **TPPP-C12** in the crystalline phase.

S8. Mesomorphic textures of TPPP-C7 and TPPP-C8

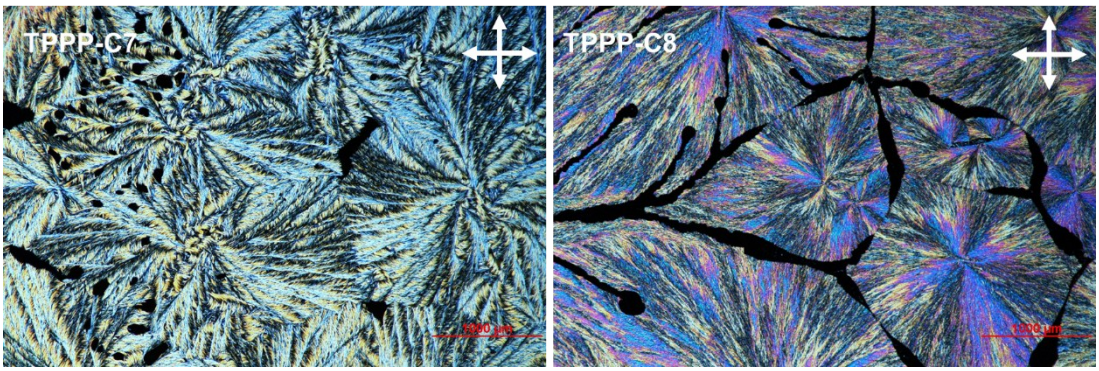

Fig. S7. Mesomorphic textures of **TPPP-C7** and **TPPP-C8** observed on cooling to 103°C and 87°C, respectively. On heating, no LC phase was detected. On cooling, LC phase was observed from their isotropic states at a cooling rate of 0.5°C/min. All textures were taken after application of a shearing force and the polarizer was in the crossed position.

S9. DSC curves of TPPP-C7 and TPPP-C8

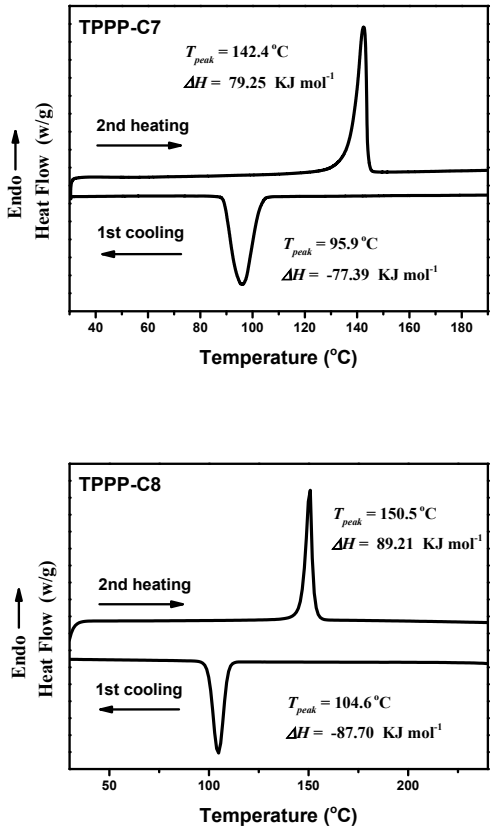

Fig. S8. DSC curves of **TPPP-C7** and **TPPP-C8** recorded under nitrogen during the first cooling and second heating cycles with a scan rate of 5°C/min.

S10. Single crystal data of TPPP-C6

Table S1. Single crystal data of TPPP-C6.

Identification code	**TPPP-C6**
Empirical formula	$C_{44}H_{46}N_2O_4$
Formula weight	666.83
Temperature/K	153.15
Crystal system	triclinic
Space group	P-1
a/Å	6.3304(13)
b/Å	7.2037(14)
c/Å	20.473(4)
α/°	89.41(3)
β/°	89.13(3)
γ/°	76.08(3)
Volume/Å^3	906.1(3)
Z	1
ρ_{calc}g/cm^3	1.222
μ/mm^{-1}	0.078
F(000)	356.0
Crystal size/mm^3	0.21 × 0.2 × 0.13
Radiation	MoKα (λ = 0.71073)
2θ range for data collection/°	5.826 to 54.968
Index ranges	$-8 \leq h \leq 8$, $-9 \leq k \leq 9$, $-26 \leq l \leq 26$
Reflections collected	12409
Independent reflections	4138 [R_{int} = 0.0704, R_{sigma} = 0.0752]
Data/restraints/parameters	4138/0/227
Goodness-of-fit on F^2	1.155
Final R indexes [I>=2σ (I)]	R_1 = 0.0638, wR_2 = 0.1427
Final R indexes [all data]	R_1 = 0.0715, wR_2 = 0.1476
Largest diff. peak/hole / e Å^{-3}	0.25/-0.24

S11. ^{1}H NMR, ^{13}C NMR and MALDI-MS spectra of the TPPP derivatives

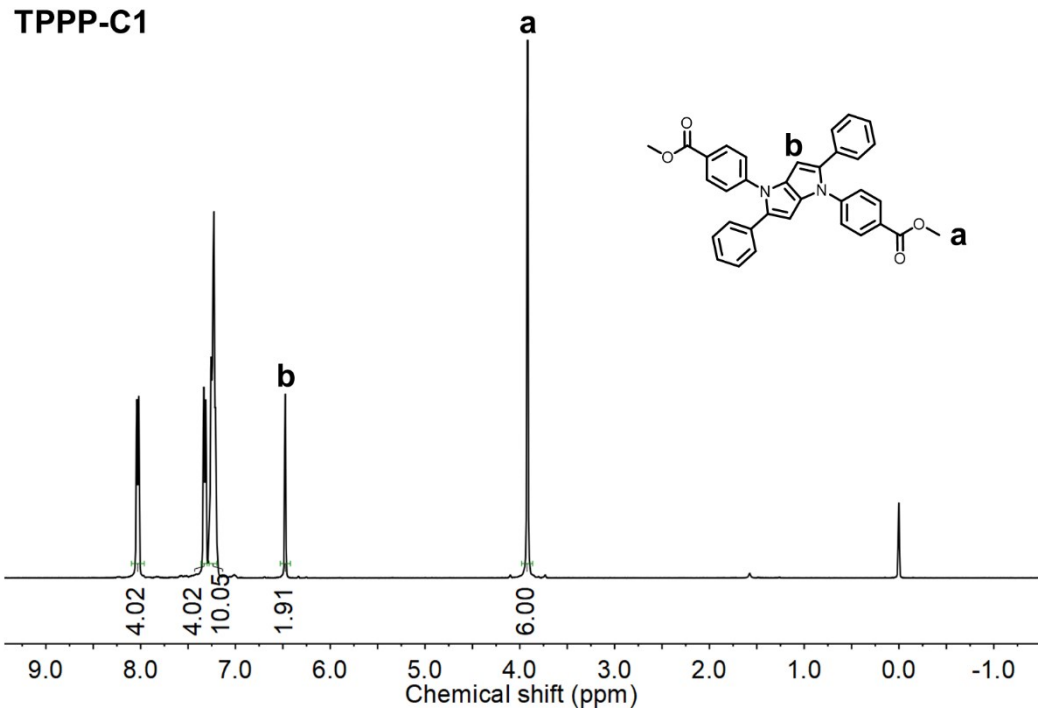

Fig. S9. ^{1}H NMR spectra of **TPPP-C1** in $CDCl_3$.

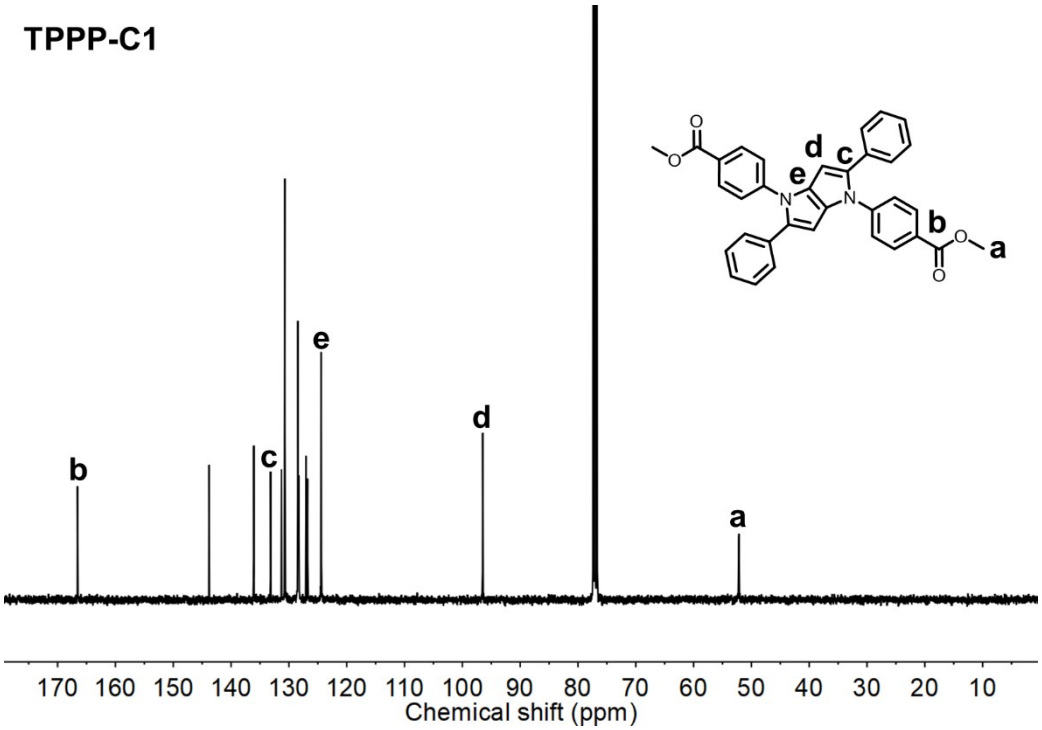

Fig. S10. ^{13}C NMR spectra of **TPPP-C1** in $CDCl_3$.

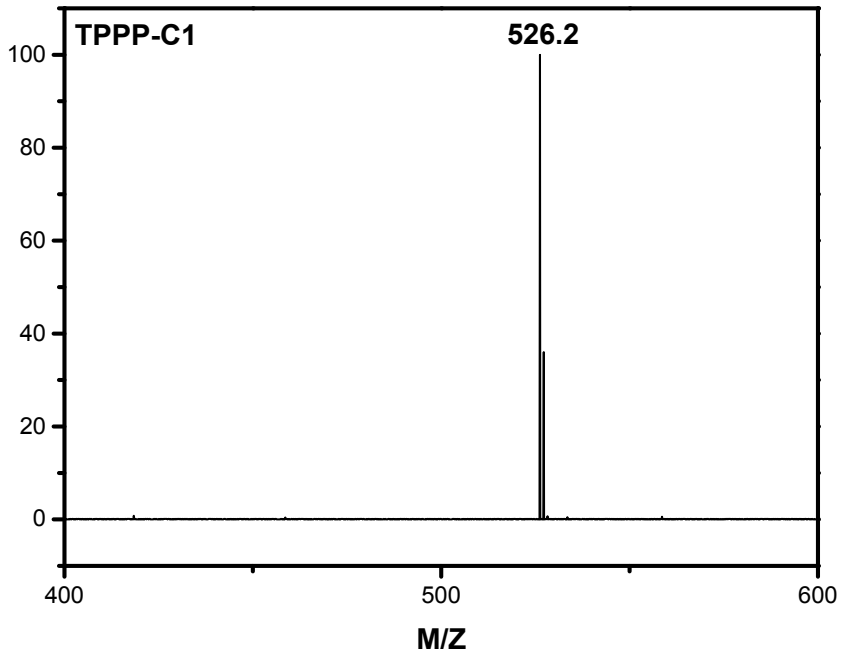

Fig. S11. MALDI-MS spectra of **TPPP-C1**.

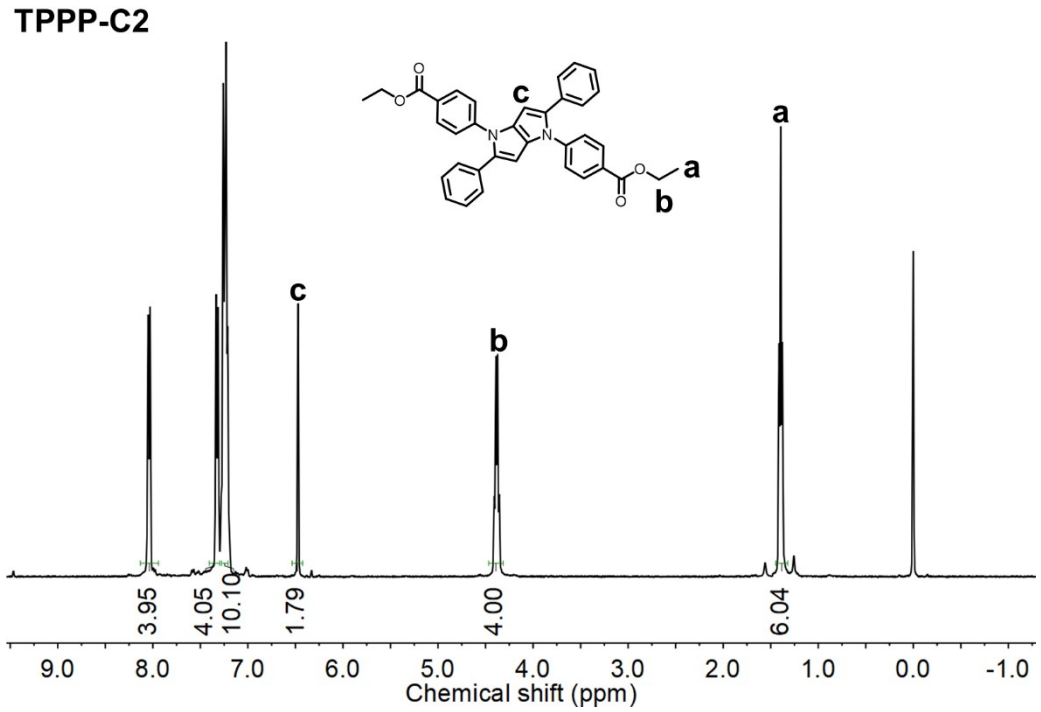

Fig. S12. ^{1}H NMR spectra of **TPPP-C2** in $CDCl_3$.

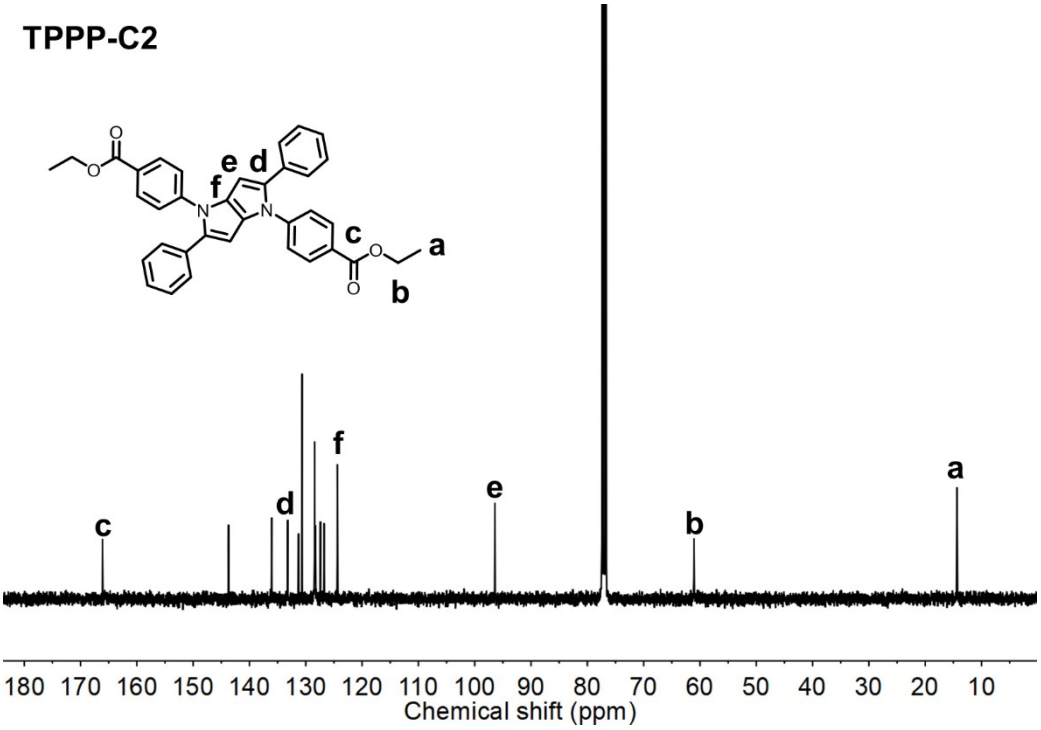

Fig. S13. ^{13}C NMR spectra of **TPPP-C2** in $CDCl_3$.

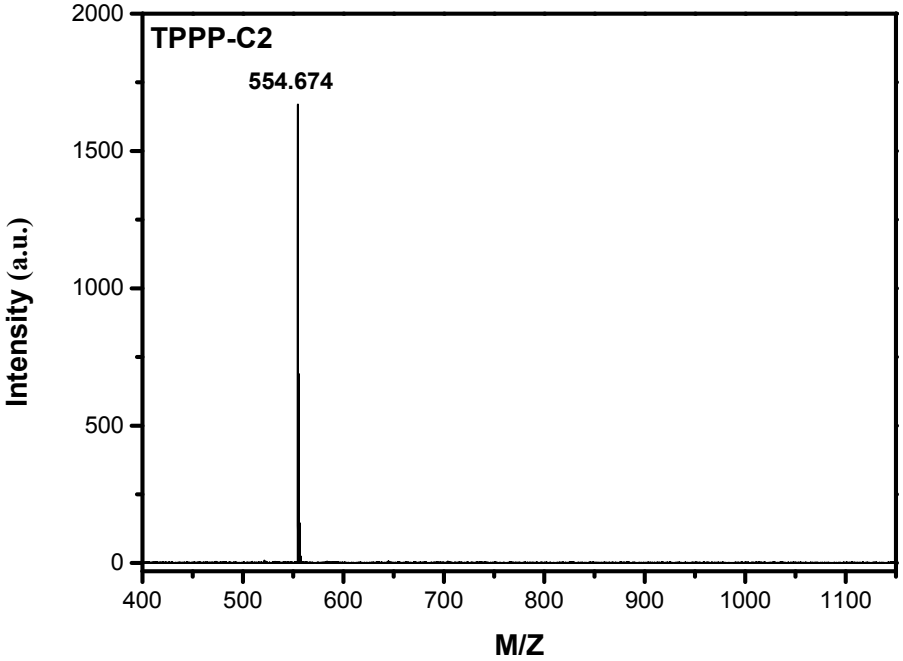

Fig. S14. MALDI-MS spectra of **TPPP-C2**.

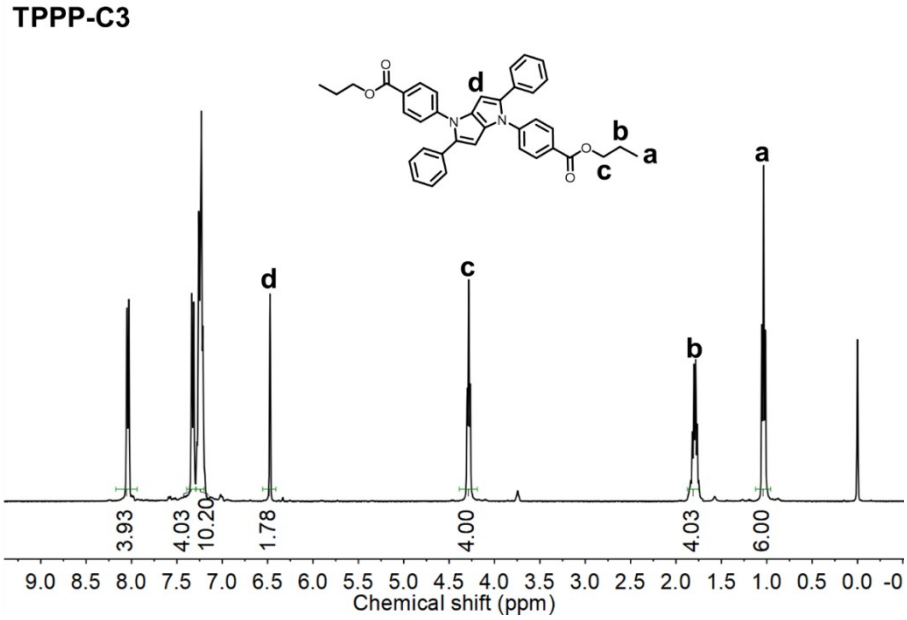

Fig. S15. ^{1}H NMR spectra of **TPPP-C3** in $CDCl_3$.

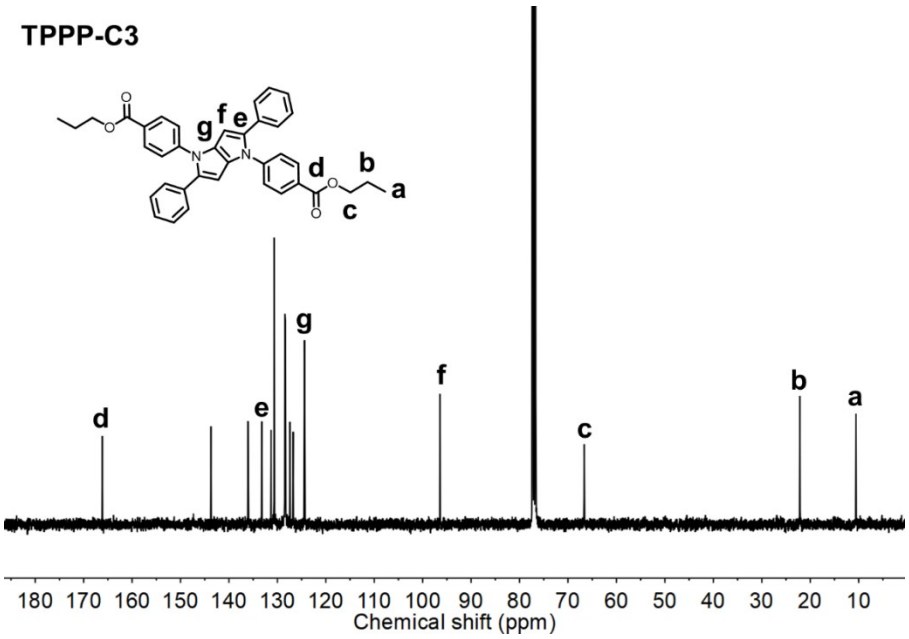

Fig. S16. ^{13}C NMR spectra of **TPPP-C3** in $CDCl_3$.

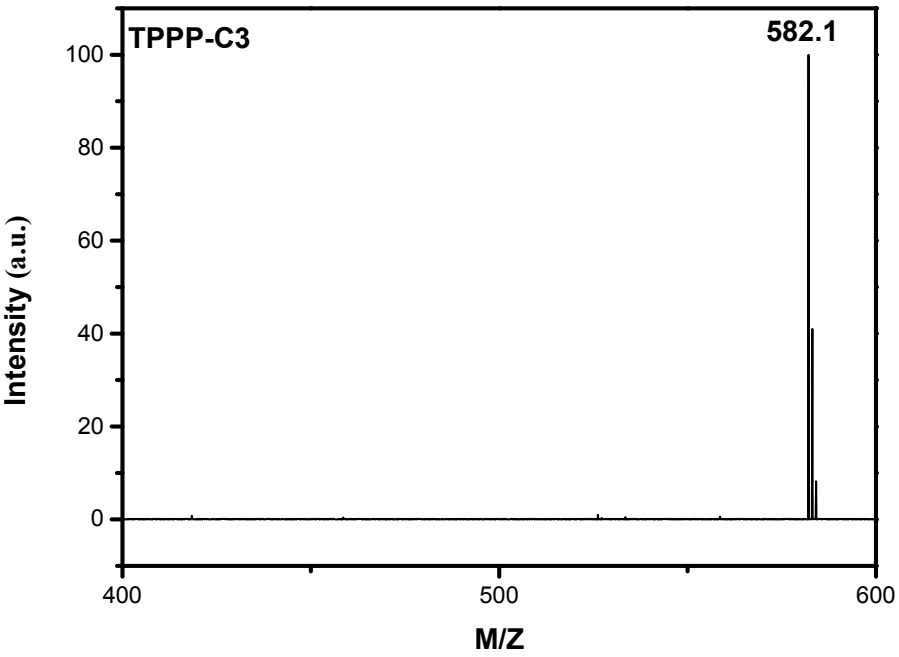

Fig. S17. MALDI-MS spectra of **TPPP-C3**.

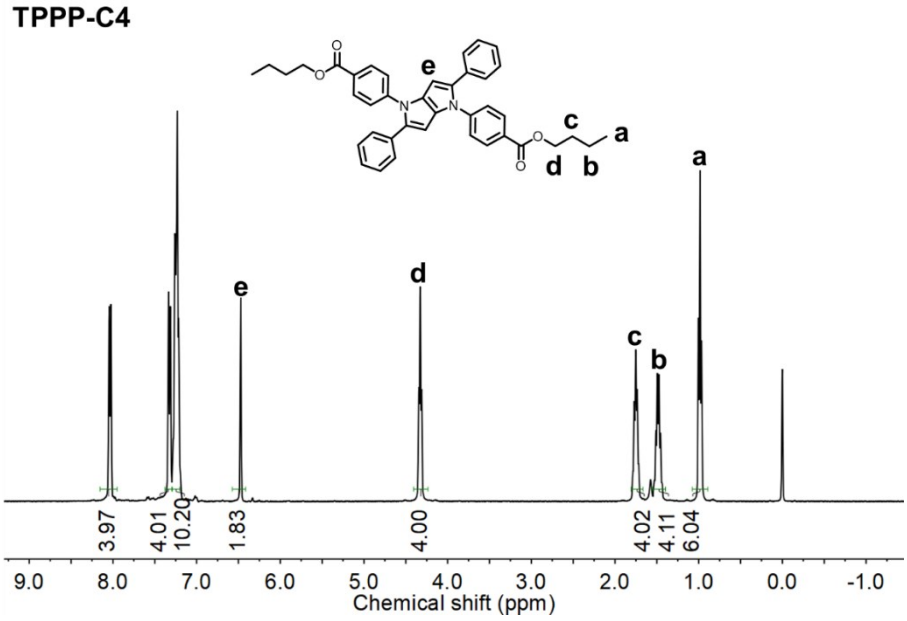

Fig. S18. ^{1}H NMR spectra of **TPPP-C4** in $CDCl_3$.

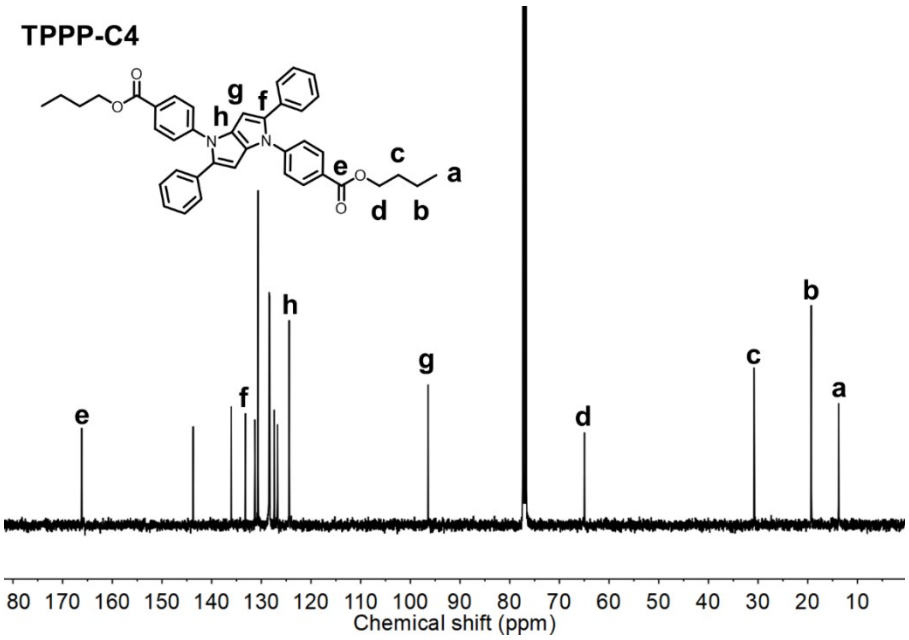

Fig. S19. ^{13}C NMR spectra of **TPPP-C4** in $CDCl_3$.

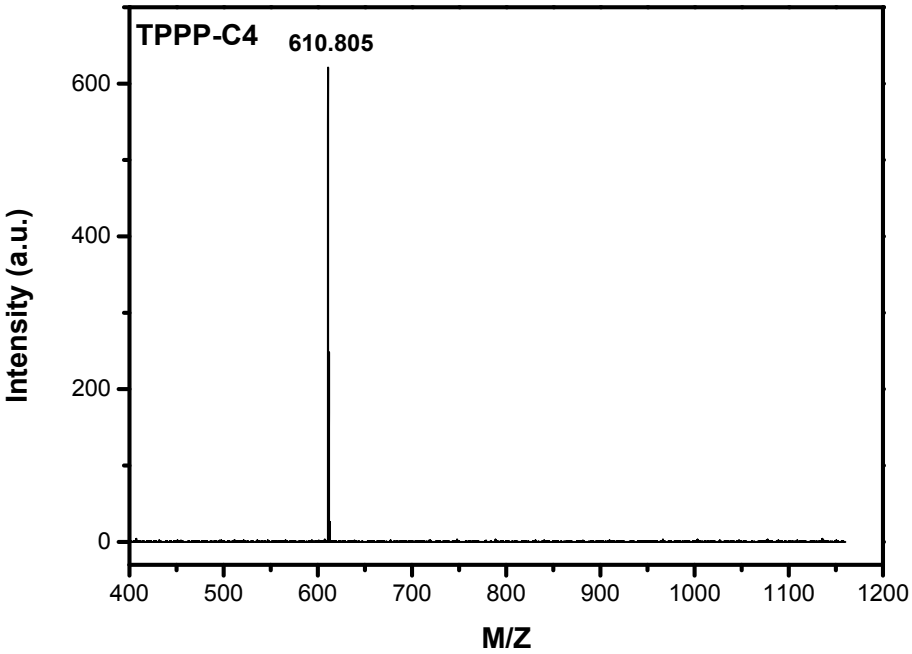

Fig. S20. MALDI-MS spectra of **TPPP-C4**.

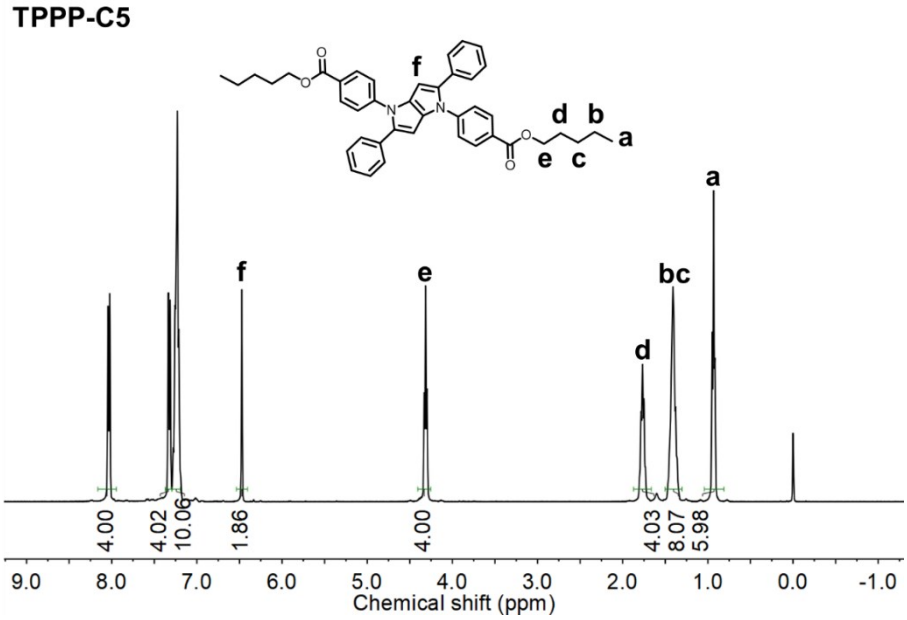

Fig. S21. ^{1}H NMR spectra of **TPPP-C5** in $CDCl_3$.

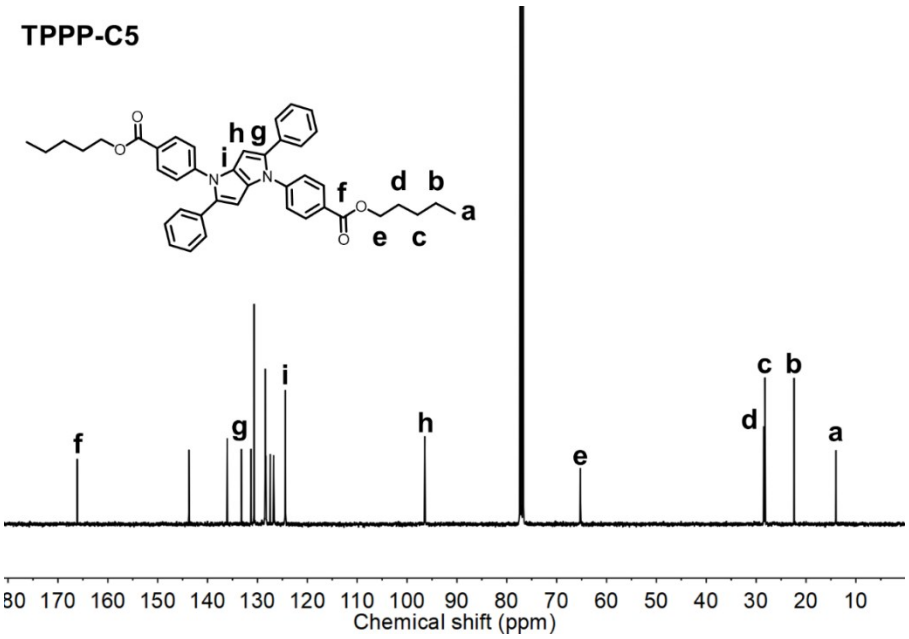

Fig. S22. ^{13}C NMR spectra of **TPPP-C5** in $CDCl_3$.

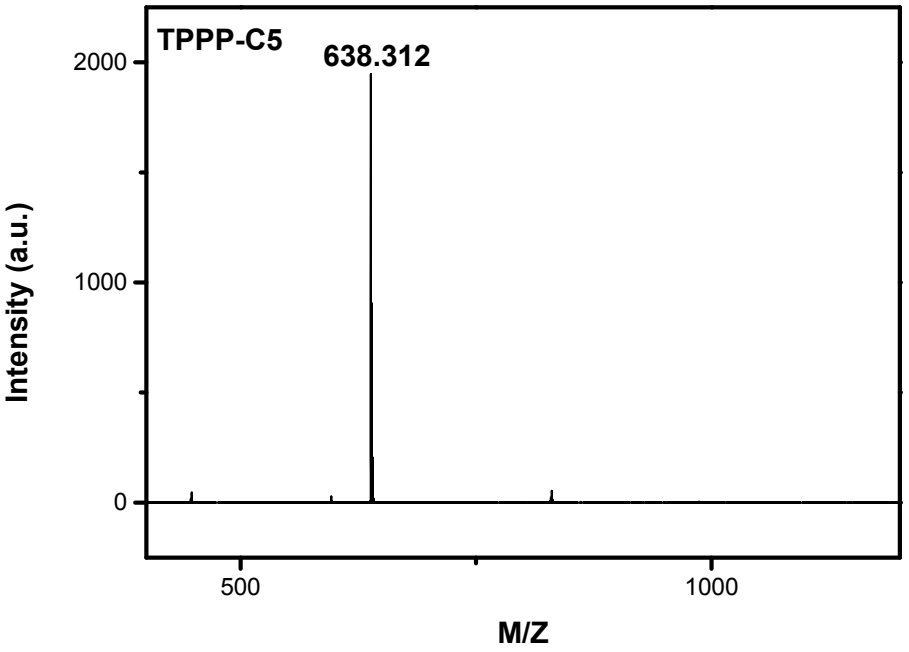

Fig. S23. MALDI-MS spectra of **TPPP-C5**.

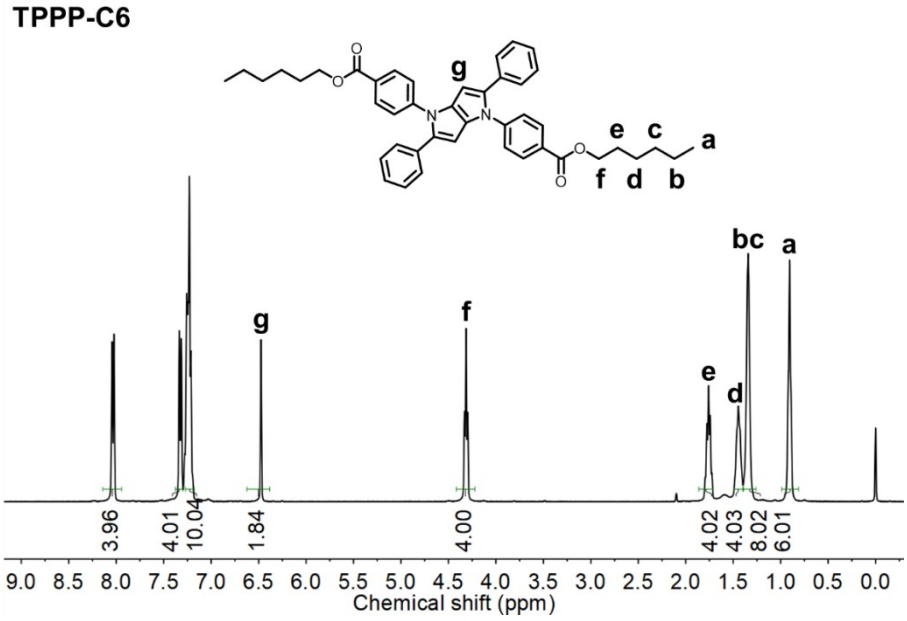

Fig. S24. ^{1}H NMR spectra of **TPPP-C6** in $CDCl_3$.

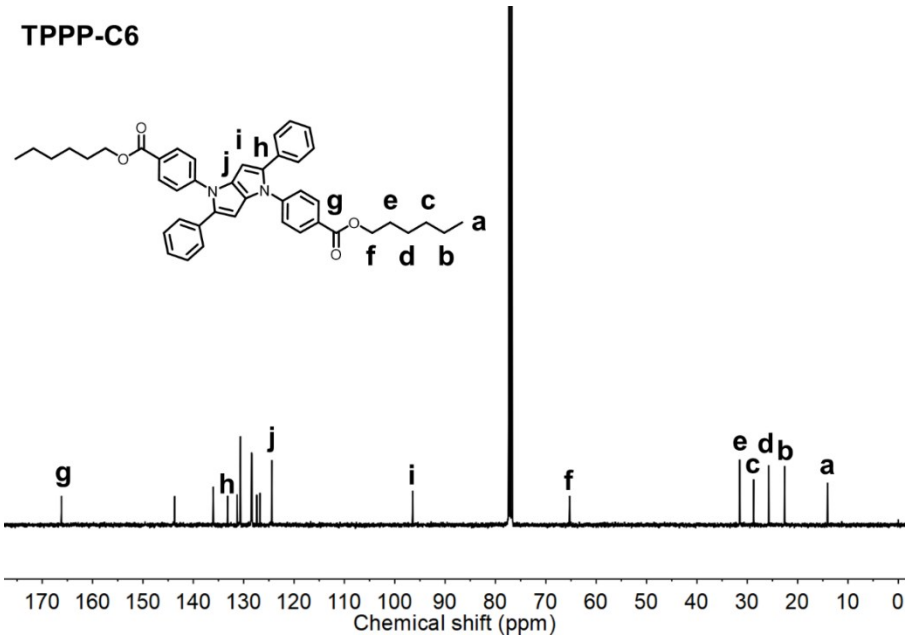

Fig. S25. ^{13}C NMR spectra of **TPPP-C6** in $CDCl_3$.

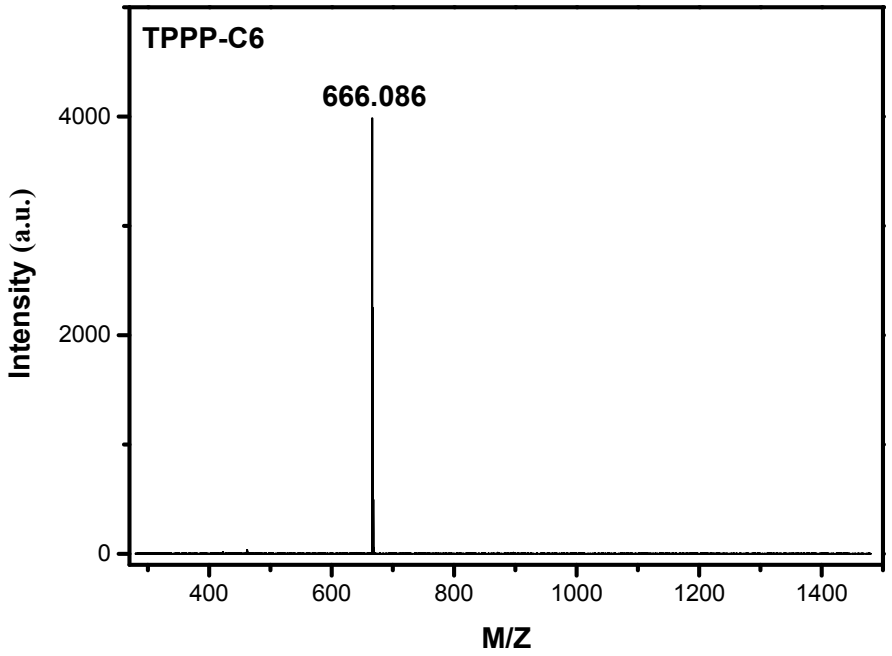

Fig. S26. MALDI-MS spectra of **TPPP-C6**.

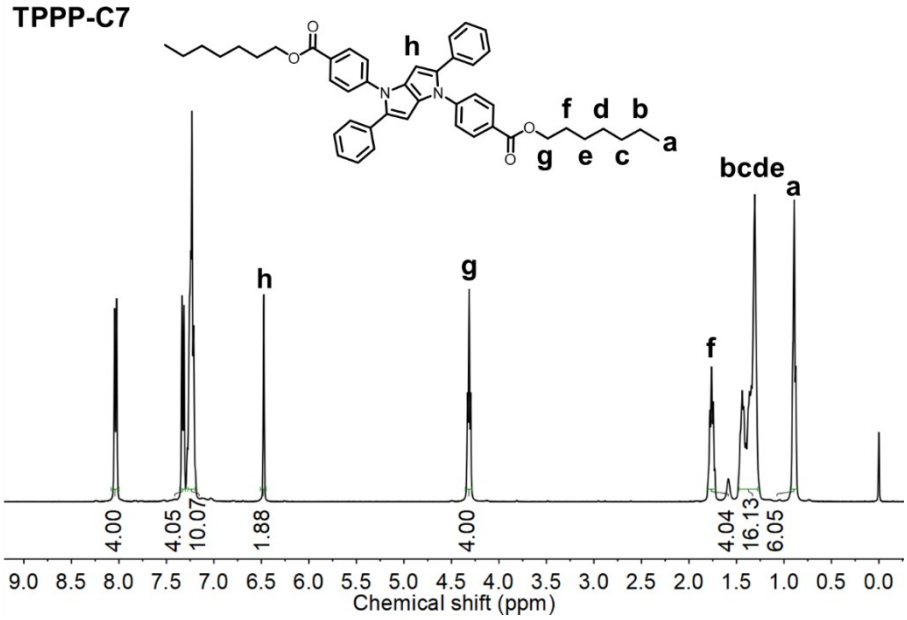

Fig. S27. ^{1}H NMR spectra of **TPPP-C7** in $CDCl_3$.

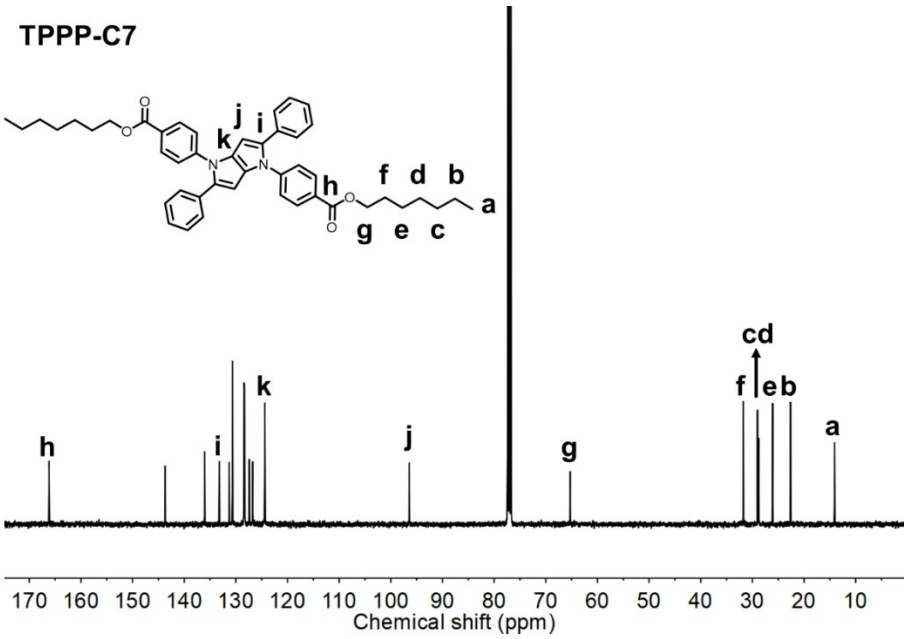

Fig. S28. ^{13}C NMR spectra of **TPPP-C7** in $CDCl_3$.

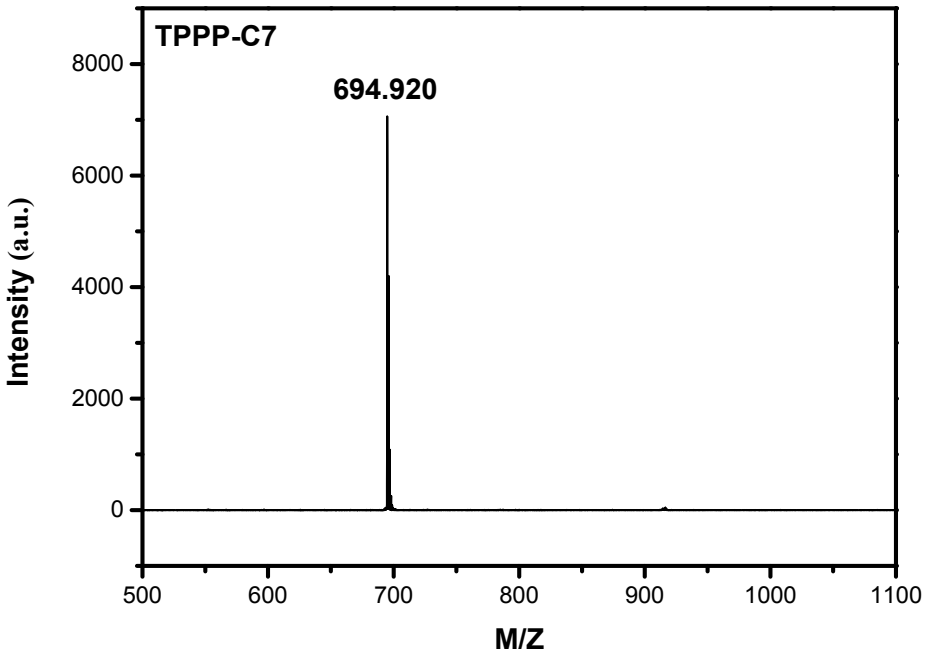

Fig. S29. MALDI-MS spectra of **TPPP-C7**.

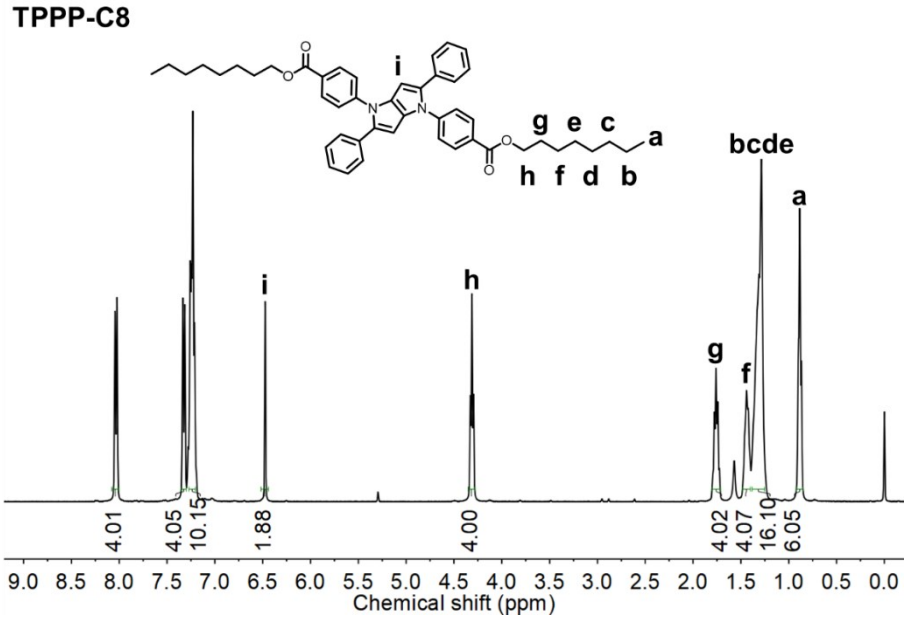

Fig. S30. ^{1}H NMR spectra of **TPPP-C8** in $CDCl_3$.

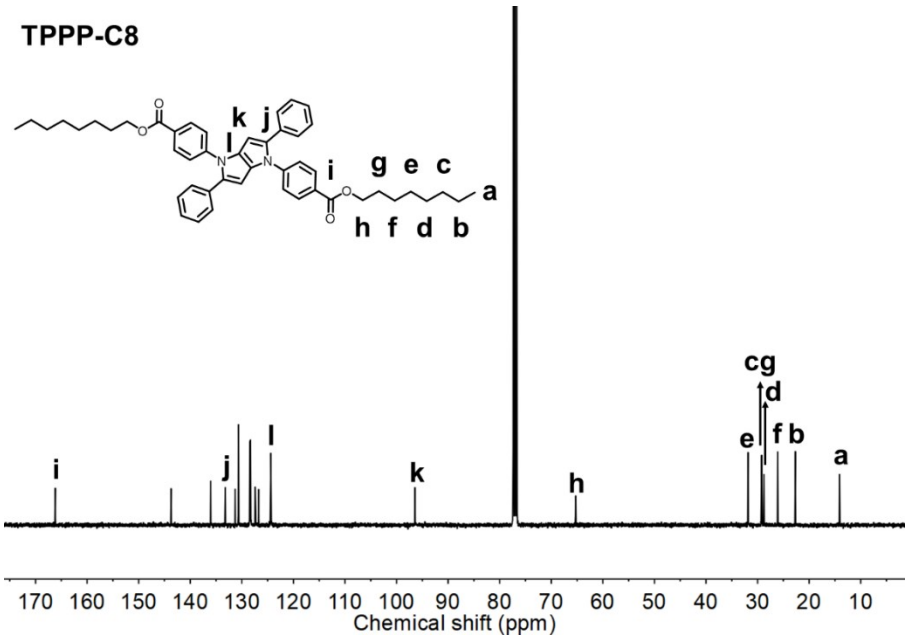

Fig. S31. ^{13}C NMR spectra of **TPPP-C8** in $CDCl_3$.

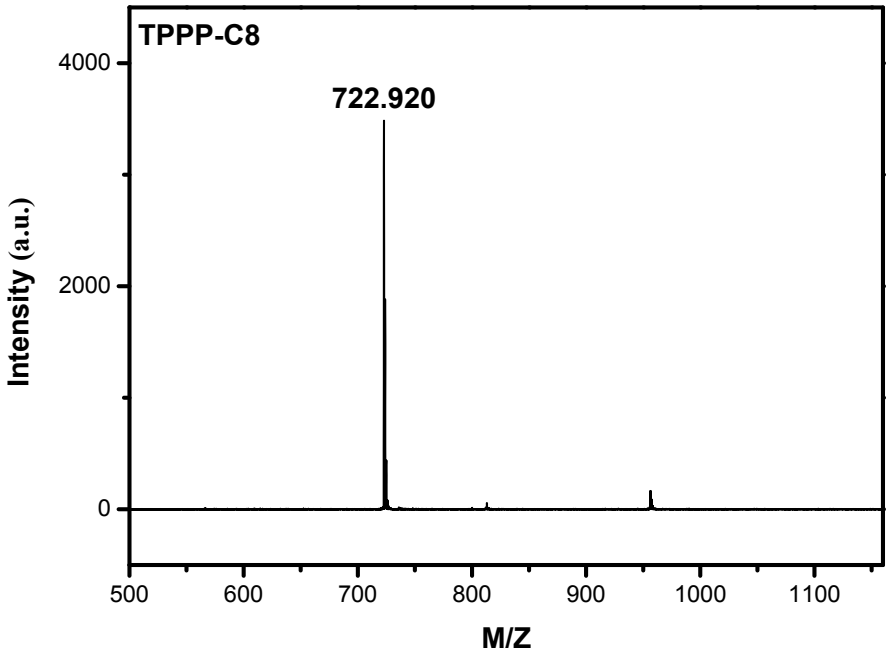

Fig. S32. MALDI-MS spectra of **TPPP-C8**.

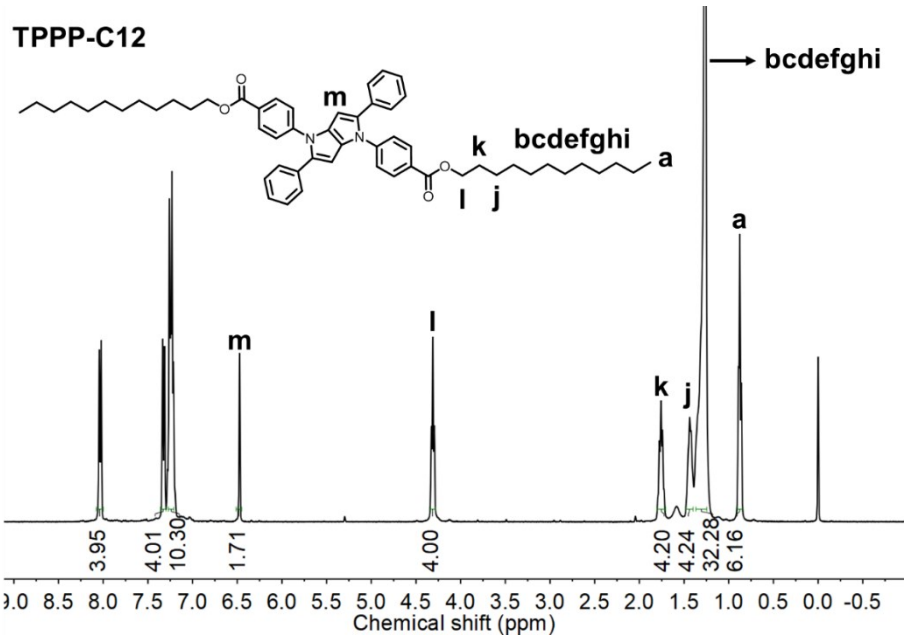

Fig. S33. ^{1}H NMR spectra of **TPPP-C12** in $CDCl_3$.

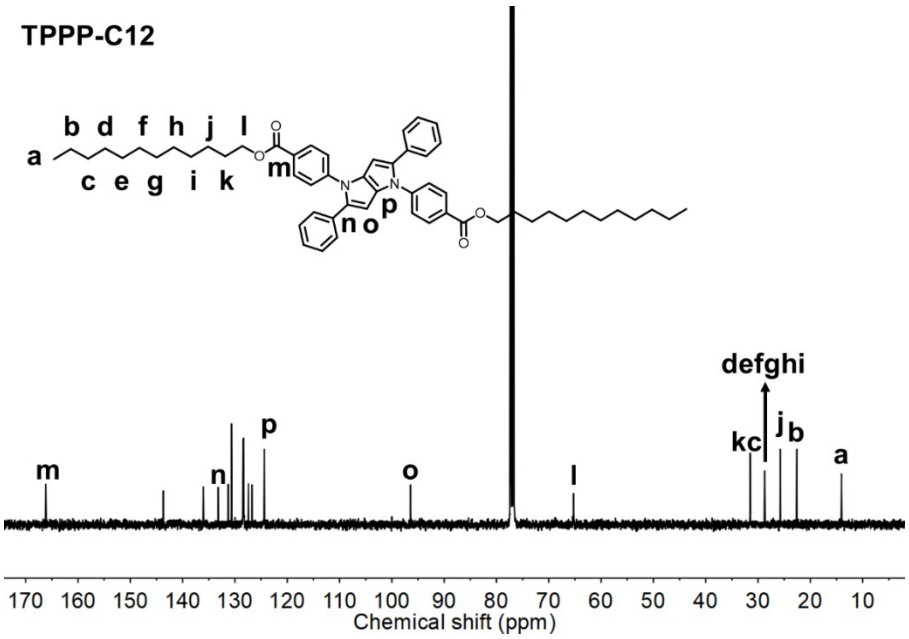

Fig. S34. ^{13}C NMR spectra of **TPPP-C12** in $CDCl_3$.

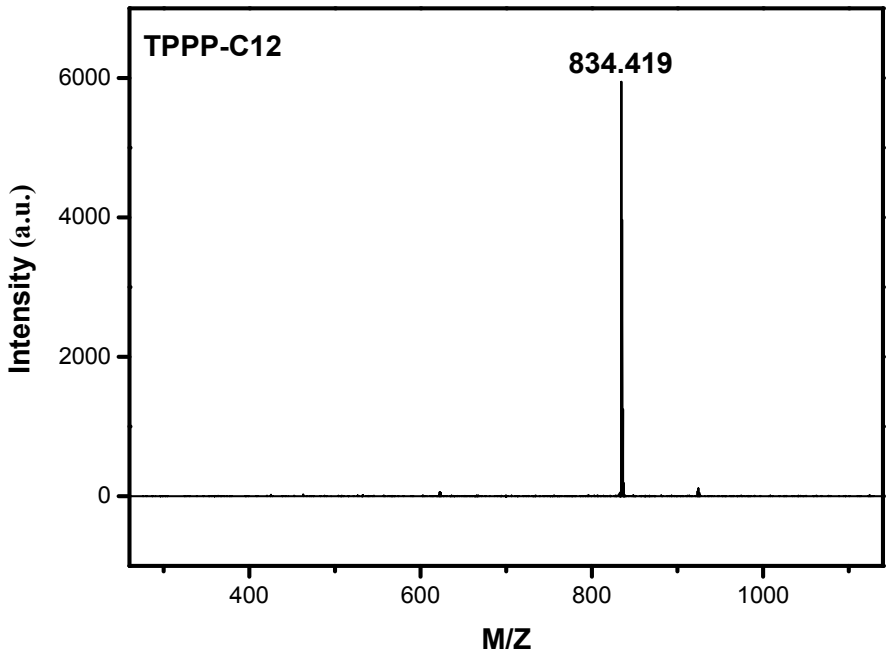

Fig. S35. MALDI-MS spectra of **TPPP-C12**.

S12. References

1 M. Krzeszewski, B. Thorsted, J. Brewer and D. T. Gryko, *J. Org. Chem.*, 2014, **79**, 3119-3128.

2 M. Krzeszewski, D. Gryko and D. T. Gryko, *Acc. Chem. Res.*, 2017, **50**, 2334-2345.